Description of ν and $\overline{\nu}$ scattering within quantum hadrodynamic theory

E. Berrueta Martinez ⬤,[1] A. Mariano ⬤,[1,2] and C. Barbero[1,2]

[1]*Departamento de Física, Facultad de Ciencias Exactas Universidad Nacional de La Plata, C.C. 67, 1900 La Plata, Argentina*
[2]*Instituto de Física La Plata CONICET, diagonal 113, 1900 La Plata, Argentina*

In this paper we develop a model to describe ν and $\bar{\nu}$ scattering in the GeV region by nuclei within a nuclear matter quantum hadrodynamics approach that is fully relativistic. We simplify it as much as possible, keeping the most relevant effects and trying to describe the greatest number of observables. We introduce explicitly the effect of ground-state correlations through a momentum distribution calculated perturbatively, and also final-state interactions using a perturbed nucleon propagator dressed by a relativistic self-energy containing nucleon-nucleon and Δ-nucleon correlations. Also, primary Δ excitations are considered within a consistent approach. All these mentioned effects are built on together, into the Lehmann representation of the propagator. Within our model we take into account the effect of 2p2h and 3p3h excitations in addition to the quasielastic 1p1h ones, needed to describe the experimental data. The obtained results are promising, showing that the model works quit well and thus putting to disposal a simple but powerful approach developed within the context of nuclear matter field theory.

I. INTRODUCTION

A. Description of quasielastic scattering

In the description of quasielastic (QE) neutrino (ν)-nucleon (N) scattering, we have three form factors (FF): (i) the $F_{1,2}(Q^2 = -(p_\nu - p_l)^2)$ vector ones [1] obtained from electron scattering using CVC, with p_ν and p_l being the neutrino and final lepton momentum, respectively; and (ii) the axial one, $F_A(Q^2)$. Assuming a dipole functional form we have $F_A(Q^2) = \frac{F_A(0)}{(1+Q^2/M_A^2)}$, where $F_A(0)$ is determined from neutron β decay [2] and the axial mass value $M_A = 1.03 \pm 0.02$ GeV is usually quoted [3]. More recently precise determinations lead to $M_A = 1.014 \pm 0.014$ [4]. With this information and a nuclear model, a description of ν and antineutrino ($\bar{\nu}$) scattering with energies around 1 GeV, should be possible with the high precision required by the new and forthcoming neutrino experiments. They are planned to measure the θ_{13} mixing angle or the leptonic CP violation and, as statistical uncertainties will diminish, the nuclear effects contributing to the systematical errors should be kept under control [5].

Current-generation [6–9] and next-generation [10,11] experiments explore a broad range of energy, and different reaction mechanisms, involving both nucleon and nuclear excitations. At hundreds of MeVs, the main mechanism is QE, where the neutrino (when we use generically "neutrinos" we refer to both neutrinos and antineutrinos) interacts primarily with individual bounded nucleons. From the experimental side, the charged current (CC) MiniBooNE data [12,13] (where ν and $\bar{\nu}$ are not monoenergetic but distributed in a flux) showed a curious result. First, if one considers only one nucleon ejection QE excitations (1p1h) the theoretical

cross sections (flux folded or unfolded) underpredict the data, where the total cross section per nucleon on ^{12}C is larger than for free ones. Second, to fit the neutrino flux folded cross section, $d\sigma/dQ^2$, within the relativistic Fermi gas model one gets $M_A = 1.35 \pm 0.17$ GeV, much larger than reported. The increase of $d\sigma/dQ^2$ with M_A also implies an important increase in the total unfolded cross section at each incident neutrino energy E_ν. The inconsistency in the impossibility of describing the MiniBooNE data with standard values of M_A, would indicate incompleteness of the considered nuclear effects and is consistent with the fact that multinucleon ejection is not distinguishable from single-nucleon production in the detectors.

An important step ahead was given in Ref. [14] with the inclusion of two-nucleon mechanisms (2p2h) and other multinucleon excitations related to the Δ resonance decay (2p2h+3p3h), to solve the mentioned paradox in describing the total QE cross section . Then, the used formalism was extended to $\bar{\nu}$ and other observables [15]. These works could reproduce the MiniBooNE total QE cross section without modifying the axial mass, suggesting that a good part of the experimental cross section was not strictly QE scattering.

Theoretical studies of npnh excitations in connection with charged current quasielastic (CCQE) at MiniBooNE kinematics were performed essentially by four groups: the works of Martini *et al.* [14,15], those of Amaro *et al.* [16,17], those of Nieves *et al.* [18,19], and the ones of Benhar *et al.* [20]. In addition, it appeared in a paper of Bodek *et al.* within a phenomenological approach related to electron scattering [21]. The models of Martini *et al.* and Nieves *et al.* are more similar: They start from a local Fermi gas picture of

the nucleus. The authors considered medium polarization and collective effects through the random phase approximation (RPA) including ph degrees of freedom, and meson exchange and gʹ Landau-Migdal parameters in the effective ph interaction. Nieves *et al.* worked within a relativistic frame while Martini *et al.* originally in a nonrelativistic one, and later improving the model through relativistic corrections. Amaro *et al.* worked out within the relativistic superscaling approach that lies on the superscaling behavior exhibited by electron scattering, without the inclusion of correlations between initial nucleons (i.e., they are distributed according to the Fermi gas model). Finally, in Benhar *et al.* the correlations of the ground state are accounted for by hole spectral functions of both nucleons.

How can we connect with the 2p2h sector? We can excite them acting with one-body currents to produce ph or Δh excitations, and then decaying into 2p1h configurations through final-state interaction (FSI) on the ejected N or by Δ decay, respectively. In an infinite system the lowest order FSI contributions give rise to divergences, as we will discuss below. The different prescriptions to regularize them lead to a model dependence of the results. Also, 2p2h are excited then by pp, Δp, or hh scattering on the 2p2h or Δhph ground-state (GS) correlations (GSC), which appear as admixtures in a perturbed GS. Finally, we can also generate 3p3h contributions through the Δ self-energy. Also, there exist several contributions from two-body currents [22], which are the so-called pion-in-flight term (PF), the contact or sea gull term (CT) and pion-pole-term (PP), as shown in Ref. [20]. We refer here only to these terms as meson exchange current contributions (MEC), but actually the most current convention consists of including the Δ-excitation terms in MEC, too.

Referring to these points, Amaro *et al.* considered only the MEC contributions and not the nucleon-nucleon (NN) correlations (GSC+FSI) and the NN-MEC interference terms. NN, MEC, and interference were present both in Martini *et al.* and Nieves *et al.* even though the first considered only Δ MEC. On the other hand, the treatment of Amaro *et al.* was fully relativistic as well as that of Nieves *et al.*, while the results of Martini *et al.* were related to a nonrelativistic reduction of the two-body currents. Amaro *et al.* considered MEC contribution only in the vector sector, while Martini *et a*l. and Nieves *et al.* considered it also in the axial one. The virtual meson exchanged in NN was just the pion for Amaro *et al.* while Martini *et al.* and Nieves *et al.* considered also the ρ-meson exchange contribution.

The inclusion of the multinucleon component has led to the agreement with the "QE" MiniBooNE data for the unfolded total cross section in all mentioned models. The same happened with Bodek *et al.*, which on the other hand agreed also with NOMAD data. Total cross section was analyzed also in the $\bar{\nu}$ mode by Martini *et al.*, Nieves *et al.*, and Bodek *et al.* The effect of npnh configurations compared to the 1p1h contribution should be somewhat less important for $\bar{\nu}$ than for ν because the spin-isospin response, which is affected by the 2p2h piece, has less weight for $\bar{\nu}$ owing to the negative axial-vector interference. This effect is evident in Martini *et al.* and Bodek *et al.*, although not in Nieves *et al.* Another important observable is the MiniBooNE flux averaged double differential cross section. This is a directly measured quantity for a given lepton energy and angle pair, E_l and θ_l, respectively, hence free from the uncertainty of neutrino energy reconstruction which is a model-dependent procedure. Calculations on 2p2h contributions have been performed by Amaro *et al.* [5,6], Nieves *et al.* [8], and Martini *et al.* [4]. Similar results were obtained by the two last groups, while in the first one the inclusion of 2p2h MEC tends to improve the agreement with data at low θ_l angles, but not sufficiently to account for discrepancies at higher angles. The absence of NN correlation might be responsible for this residual disagreement.

B. A relativistic model for nuclear matter

After a short review on the state of art, we will describe our model for neutrino-nucleus scattering which is in short, a model developed within a quantum hydrodynamics frame for nuclear matter (QHDI) with inclusion of pion (π) ring series. The nonrelativistic approximations (NR) are deficient in several ways as was discussed, for example, for electron scattering [23]. Higher-order terms in the NR reduction procedure may become important when the momentum transfer $|\mathbf{q}|$ becomes comparable to the nucleon mass m_N. In NR it is tacitly assumed that the $\frac{q_0}{m_N} \ll 1$, q_0 being the energy transfer to the nucleus. This holds for elastic scattering and excitation of low-lying levels but is certainly not the case on the high-energy side of the QE peak. Retardation effects are not accounted for, and one might expect that invariant FF, $F_1(Q^2)$, $F_2(Q^2)$, should to be used rather than the three-dimensional Fourier transform of charge and magnetization densities. In NR explicit mesonic degrees of freedom are eliminated. Thus, not only is π production above the π threshold omitted but also meson-exchange corrections to QE electron scattering. All these difficulties, which also are present in neutrino scattering, are closely related and require in principle a consistent relativistic (R) theory of nuclei. If the nucleons inside the nucleus obey a relativistic wave equation, one has to specify the transformation properties of the potentials. For example, it is well known they give rise to important effects even at low energies: a strong nuclear spin-orbit force and an energy dependence of the real part of the optical potential [24]. Also, the role played by relativistic kinematics is important for describing the double differential cross section, because the momenta and energies involved in these neutrino reactions are somewhat large. For the MiniBooNE case, the neutrino energy extends to 2 GeV and the ejected N kinetic energy in the QE process can be a few hundred MeV making a NR approximation questionable. Finally, it was pointed out that conclusions on the role of the multinucleon process are doubtful within a NR framework [15].

A simple but consistent relativistic framework fulfilling all the properties listed above, is provided by a nuclear field theory from Walecka which incorporates the interaction of the N with the σ and ω meson fields (QHDI) [25]. In spite of successful treatments with the QHDI in describing QE, inelastic, and scaling effects [23,26,27], we note the absence of the pionic degree of freedom in the commonly used mean field

theory (MFT) or relativistic Hartree (RHA) and Hartree-Fock (RHF) approximations within QHDI. This is curious, because π mediate the NN interaction at all but to shortest ranges. Furthermore, chiral symmetry is an important approximated symmetry of strongly interacting systems which requires pionic degrees of freedom.

Properties of N propagation in the presence of the nuclear π field was not extensively studied in relativistic field theory models. There are some related works, but these are based on NR formalisms. To obtain a model that maintains chiral symmetry and achieves nuclear-matter saturation it is necessary to include terms beyond the MFT. Also it is important to include Δ isobars in addition to N because 2π exchange (TPE) correlated with intermediate Δ's supply important mid-range attraction in NN scattering. Relativistic chiral treatments of nuclear matter were achieved studying the pion-ring series [28] and second-order one-π exchange with π propagation modified by the nuclear medium. The adopted Lagrangian incorporates the physics of the original Walecka QHDI model plus PCAC (partial conservation of axial-vector current), the nonlinear $\sigma\pi$ interaction, and Δ contributions to the πN interaction. In summary, in addition to the QHDI we will include a dressed π exchange and TPE correlated contributions, which have consequences described as follows.

For the intermediate-range NN force, TPE correlated or uncorrelated, are known to dominate. In nuclear matter, TPE's effects on the binding energy are expected to be even more important than the second-order 1π exchange (OPE) mainly because of the presence of the Δ isobars. In addition, π propagation in the nuclear medium can generate a collective spin-isospin modes by coupling to the ph and Δh states. Without the short-range correlations between baryons, the collective spin-isospin mode would develop into a so-called pion condensate even at normal densities. If π propagation in the nuclear medium is modified so as to excite collective modes, the effects of the uncorrelated TPE and the second-order OPE on the binding energy of nuclear matter should be enhanced correspondingly. In other words, the exchanged pions between nucleons can be rescattered by other N, thus amplifying the attractive nuclear force. In Ref. [28] the single-particle nature of N in relativistic nuclear matter was studied by calculating its self-energy in the presence of the pion-ring series. Thus, despite the fact that now σ (which interacts with π) provides only a small shift of the effective Dirac mass, the new π effects cause an additional shift. In addition, if we include TPE and OPE contributions [29], the N self-energy gives one a way of introducing the FSI between 1p1h and 2p2h excitations fully relativistically and to all orders within the perturbed propagator. The mentioned formalism plus GSC involved in a momentum distribution calculated perturbatively onto a 2p2h+4p4h space [30], will be used to describe the mentioned observables in neutrino-nucleus scattering. We get a good description as described below.

The paper will be ordered as follows: In Sec. II we present the ingredients of our model; in Sec. III we present calculations and results; and finally in Sec. IV we sketch our conclusions.

II. NEUTRINO(ANTINEUTRINO) NUCLEUS SCATTERING

We start with the cross section for the $\nu(\bar{\nu})A \to \mu(\mu^+)N'A'$ process in the LAB system, where $k_A = (M_A, \mathbf{0})$, $k_{\nu \equiv \nu, \bar{\nu}} = (E_\nu, E_\nu \hat{\mathbf{k}})$, and $p_{l \equiv \mu \mu^+} = (E_l = \sqrt{p_l^2 + m_l^2}, p_l \sin\theta_l \cos\phi_l, p_l \sin\theta_l \sin\phi_l, p_l \cos\theta_l)$:

$$\frac{d\sigma_{\nu A}}{dT_l d\cos\theta_l}$$
$$= \frac{\Omega_A}{2E_\nu} \frac{1}{2} \sum_{m_{s_\nu}} 2\text{Im}\big[\mathcal{M}(k_\nu m_{s_\nu} T_l \theta_l \to k_\nu m_{s_\nu} T_l \theta_l)\big], \quad (1)$$

$$2\text{Im}\big[\mathcal{M}(k_\nu T_l \theta_l \to k_\nu T_l \theta_l)\big]$$
$$= \sum_{m'_s s \, m'_t s} \left(\int \frac{d\Phi_l}{(2\pi)^3} \prod_{i=1}^{n} \mathcal{N}_l \int \frac{d^3 p_i}{(2\pi)^3} \mathcal{N}_{p_i} \frac{d^3 k_i}{(2\pi)^3} \mathcal{N}_{k_i} \right)$$
$$\times |\mathcal{M}(k_\nu k_1 k_2 ... \to p_l p_1 p_2 ...)|^2$$
$$\times (2\pi)^4 \delta^4(p_l + p_1 + p_2 ... - k_\nu - k_1 - k_2 - ...),$$
$$(2)$$

$$\xi \equiv p_l, p_i, k_i, \ \xi = (E(\boldsymbol{\xi}), \boldsymbol{\xi}), \ \mathcal{N} = \frac{m^2}{\sqrt{\boldsymbol{\xi}^2 + m^2}},$$

$$\boldsymbol{\xi} \equiv \mathbf{k}_l, \mathbf{k}_i, \mathbf{p}_i, \ m \equiv m_l, m_N, \quad (3)$$

where in Eq. (2) the spin (m_s) and isospin (m_t) projections were omitted in the amplitudes $\mathcal{M}$. Here Ω_A is the nucleus volume so the density reads $\rho_A = \frac{A}{\Omega_A} = \frac{2k_F^3}{3\pi^2}$ with k_F the Fermi momentum. $T_l = E_l - m_l$ is the lepton kinetic energy, and we have assumed that the final nuclear states are npnh configurations (not pions in final state are considered here) excited from the GS being initial(final) nucleon momentum indicated with k_i (p_i). Amplitudes will be schematized considering that initial particles are represented as backward lines in Feynman graphs. Note that Eq. (2) is the optical theorem applied to the considered process, and it is valid if we include in $\mathcal{M}(k_\nu T_l \theta_l \to k_\nu T_l \theta_l)$ *all* npnh intermediate contributions. We will proceed choosing a determined 1p1h, 2p2h, etc., intermediate state and evaluating its contribution to $\mathcal{M}(k_\nu T_l \theta_l \to k_\nu T_l \theta_l)$ through the Feynman rules in quantum hadrodynamic, as developed in the next subsections.

A. Perturbed nucleon propagator

We will need to evaluate contributions to $\text{Im}[\mathcal{M}(k_\nu T_l \theta_l \to k_\nu T_l \theta_l)]$, the relativistic perturbed N propagator for infinite nuclear matter. The unperturbed N propagator S_N^0 in nuclear matter reads

$$S_N^0(p) = \frac{(\not{p} + m_N)}{2E(\mathbf{p})}\left[\frac{(1 - \theta(E_F - p^0))}{(p^0 - E(\mathbf{p})) + i\epsilon} + \frac{\theta(E_F - p^0)}{(p^0 - E(\mathbf{p})) - i\epsilon}\right],$$
$$(4)$$

being $E(\mathbf{p}) = \sqrt{\mathbf{p}^2 + m_N^2}$ and where the negative energy contribution was not included. The Heaviside function $\theta(E_F - (p^0 = E(\mathbf{p}))) = \theta(k_F - p)$ is the momentum distribution of

the unperturbed ground state normalized as

$$\int d^3k C\theta(k_F - |\mathbf{k}|) = A/4, \ C = \Omega_A/(2\pi)^3 = \frac{3A}{16\pi k_F^3}. \tag{5}$$

The interaction of N with other N' is introduced in nuclear matter through a self-energy that from covariance should be written as $\Sigma_N(p) = I\Sigma^s(p) - \gamma_\mu\Sigma^\mu(p) = \Sigma^s(p) - \gamma_0\Sigma^0(p) + \boldsymbol{\gamma}.\mathbf{p}\Sigma^v(p)$, where Σ^s and Σ^v are the scalar and vector contributions [25]. Usually by rotational invariance in nuclear matter or spin-zero nuclei we can take $\Sigma^i(p) = 0$ ($\Sigma^v = 0$). Then, the perturbed S_N propagator should be obtained as usual by solving the Dyson equation [31],

$$S_N^{-1} = S_N^{0-1} - \Sigma_N \Rightarrow S_N = S_N^0 + S_N^0\Sigma S_N = S_N^0 + S_N\Sigma_N S_N^0, \tag{6}$$

and it is achieved by using the Lehmann spectral representation [31] for the propagator,

$$S_N(p) = \int_{-\infty}^{+\infty}\left[\frac{A_p(\omega, \mathbf{p})}{p^0 - \omega + i\eta} + \frac{A_h(\omega, \mathbf{p})}{p^0 - \omega - i\eta}\right]d\omega, \tag{7}$$

where p, h indicates particle and hole states regarding k_F. As shown in detail in Ref. [29], one gets

$$S_N(p) = \frac{\tilde{\not{p}} + \tilde{m}_N}{\tilde{p}^2 - \tilde{m}_N^2 + i\,\mathrm{sgn}(\mathrm{Re}[\tilde{p}^0])\mathrm{sgn}(p^0 - E_F)\epsilon}, \tag{8}$$

where $\tilde{p}^\mu = (p^0 + \Sigma^0(p), \mathbf{p}(1 + \Sigma^v(p)))$ is the nucleon perturbed momentum and $\tilde{m}_N(p) = m_N + \Sigma^s(p)$ its effective mass, where the modifications introduced by the self-energy are evident. Note that the unperturbed propagator (4) is recovered by making $\Sigma_N \equiv 0 \Rightarrow \tilde{p} \to p^\mu$, $\tilde{m}_N(p) \to m_N$ in Eq. (8).

The structure of the self-energy components depend on the specific contributions considered to be built it. We can include binding effects, FSI, π production, etc., through Σ_N. However, we can still get some general results by rearranging the denominator in Eq. (8) as

$$\tilde{p}^2 - \tilde{m}_N^2 = (p^0 + \mathrm{Re}\Sigma^0 - \tilde{E}(p))(p^0 + \mathrm{Re}\Sigma^0 + \tilde{E}(p))$$
$$- 2i\tilde{m}_N\left(\mathrm{Im}\Sigma^s - \frac{(p^0 + \mathrm{Re}\Sigma^0)}{\tilde{m}_N}\mathrm{Im}\Sigma^0\right), \tag{9}$$

where we drop $\mathrm{Im}(\Sigma^{0,s})^2$ and make $\tilde{m}_N(p) \approx m_N + \mathrm{Re}\Sigma^s(p)$. Equating (9) to zero we found the pole solutions, $E(p)^\pm = \pm\tilde{E}(p) - \mathrm{Re}\Sigma^0(p)|_{p^0 = E(p)^\pm}$ with $\tilde{E}(p) = \sqrt{\mathbf{p}^2 + \tilde{m}_N^2}$. Then, developing the real self-energy parts around $p^0 = E^+$ and keeping terms to first order we get

$$\tilde{p}^2 - \tilde{m}_N^2 \approx Z_\mathbf{p}^{+-1}(p^0 + \mathrm{Re}\Sigma^0(E^+) - \tilde{E}(E^+))$$
$$\times (p^0 + \mathrm{Re}\Sigma^0(E^+) + \tilde{E}(E^+))$$
$$- 2i\tilde{m}_N(E^+)\left(\mathrm{Im}\Sigma^s(p^0) - \frac{\tilde{E}(E^+)}{\tilde{m}_N(E^+)}\mathrm{Im}\Sigma^0(p^0)\right), \tag{10}$$

$$Z_\mathbf{p}^{+-1} = \left(1 - \frac{\tilde{\mathbf{p}}^2}{\tilde{E}}\partial_0\mathrm{Re}\Sigma_v - \frac{\tilde{m}_N}{\tilde{E}}\partial_0\mathrm{Re}\Sigma_s + \partial_0\mathrm{Re}\Sigma^0\right)_{p^0 = E^+}. \tag{11}$$

Now, if we make the approach $E^+ \approx \tilde{E}(k_F, \Sigma(E_F)) - \mathrm{Re}\Sigma^0(E_F) = E_F$, this defines the Fermi energy. Developing self-energy imaginary parts around it, we get

$$\mathrm{Im}\Sigma^s(p^0) - \frac{\tilde{E}(k_F)}{\tilde{m}_N(E_F)}\mathrm{Im}\Sigma^0(p^0)$$
$$\approx -1/2[a^0 - a^s](p^0 - E_F)^2$$
$$\equiv \begin{cases} -\Gamma_N(p)/2Z_\mathbf{p}^+, \ p^0 > E_F \\ \Gamma_N(p)/2Z_\mathbf{p}^+, \ p^0 < E_F, \end{cases} \tag{12}$$

where $a^{0,s}$ and $Z_\mathbf{p}$ depend on the detailed contributions present in the self-energy. Finally, introducing Eqs. (10)–(12) in (8) we get an approximation ready to perform the calculations:

$$S_N(p) = (\not{p} + m_N)\theta(p^0)\left[\frac{Z_\mathbf{p}^+(1 - \theta(E_F - p^0))}{p^{02} - \tilde{E}^2 + i\tilde{m}_N\Gamma_N(p)}\right.$$
$$\left. + \frac{Z_\mathbf{p}^+\theta(E_F - p^0)}{p^{02} - \tilde{E}^2 - i\tilde{m}_N\Gamma_N(p)}\right], \tag{13}$$

$$\Gamma_N(p) = Z_\mathbf{p}^+[a^0 - a^s](p^0 - E_F)^2, \tag{14}$$

where the real self-energy parts are evaluated at E_F. As we will see, $\mathrm{Re}[\Sigma^0(E_F)]$ varies slowly around $p = k_F$ and thus, to simplify the calculation, we make the approach $\tilde{E}(p, \tilde{m}_N) - \mathrm{Re}[\Sigma^0(E_F)] \approx \tilde{E}(p, \tilde{m}_N')$, being $\tilde{m}_N'$ fixed at $p = k_F$. Because usually $\mathrm{Re}[\Sigma^0(E_F)] < 0$, we have $\tilde{m}_N' > \tilde{m}_N$. This approach is useful because it leads to $p^2 = \tilde{m}_N'^2$ as for an on-shell nucleon, avoiding any complication when one needs to make transformations to other frames different from the LAB one. Now, from here and on, we understand $\tilde{E} \equiv \tilde{E}(p, \tilde{m}_N')$, $\tilde{m}_N \equiv \tilde{m}_N'$ in the calculations. For our calculations we need to look for the Lehmann representation (7) of the approximated propagator from Eq. (13), for which we get

$$A_{p/h}(p^0, \mathbf{p}) \approx \frac{1}{\pi}\frac{\theta(p^0)(\not{p} + \tilde{m}_N)\tilde{m}_N\Gamma(p^0)}{(p^{02} - \tilde{E}^2)^2 + (\tilde{m}_N\Gamma_N(p^0))^2}\begin{cases} 1 - n(p) \\ n(p) \end{cases},$$
$$\Gamma_N(p_0) = \begin{cases} 1 - n(\mathrm{p}) \\ n(p) \end{cases}[a^0 - a^s](p^0 - E_F)^2, \tag{15}$$

where we identify $Z_\mathbf{p}^+\theta(E_F - p) \equiv n(p)$, $Z_\mathbf{p}^+\theta(p - E_F)) \equiv 1 - n(p)$, $n(p)$ fulfilling Eq. (5) changing $\theta(k_F - p) \to n(p)$. From Eqs. (11) and (12) we see how Σ_N introduces naturally GSC and a width Γ_N that modulates the contributions of the momenta regards Fermi level. From now and on we use $\tilde{p} \equiv p = (\tilde{E}, \mathbf{p})$ to simplify expressions.

B. QE with 1p1h contributions

We begin with the QE response with 1p1h final states. For ν scattering and when only $n = 1$ is considered in Eq. (2), we have the amplitude shown in Fig. 1. For $\bar{\nu}$ scattering the changes $n, p, W^+ \to p, n, W^-$ must be done. This amplitude is built in the Appendix, and after using trace technics and integrations of time momentum components

we get

$$
2\mathrm{Im}\sum_{m_v}\mathcal{M}_{1p1h} = \frac{16}{(2\pi)^5}\left(\frac{G_F}{\sqrt{2}}\right)^2 \cos^2\theta_c \tilde{m}_N \tilde{m}_{N_f}\int dk^3\int dE_l d\cos\theta_l \int d\phi_l p_l \theta(E_l - E_\nu)L_{\mu\nu}
$$

$$
\times \sum_{m's}\bar{u}(k+q,m')(-i)\sqrt{2}\hat{J}_H^\mu(q)u(k,m)\left[\bar{u}(k+q,m')(-i)\sqrt{2}\hat{J}_H^\nu(q)u(k,m)\right]^*
$$

$$
\times \int_{E_{\min}}^{E_F}\frac{\tilde{m}_{N_f}\Gamma_N(\omega+q_0)(1-n(\mathbf{k}+\mathbf{q}))}{\pi((\omega+q_0)^2 - \tilde{E}(\mathbf{k}+\mathbf{q})^2)^2 + \left(\tilde{m}_{N_f}\Gamma_N(\omega+q_0)\right)^2}\frac{\tilde{m}_N\Gamma(\omega)n(\mathbf{k})}{\pi((\omega)^2 - \tilde{E}(\mathbf{k}))^2)^2 + (\tilde{m}_N\Gamma_N(\omega))^2}d\omega, \quad (16)
$$

with $\omega_{\min} = \max(0, E_F - q_0)$. Note that we have introduced naturally GSC through the occupation numbers and that we can have contributions from initial N with $k > k_F$ and with final ones with $p < k_F$, because now they have certain width. We will return to this below. We have included $\tilde{m}_N$ and $\tilde{m}_{N_f}$ with different values to account for the separation energy between the initial and final nuclei.

Until this moment we have not mentioned any model to calculate Σ_N in nuclear matter. We will begin to develop it for the QE 1p1h case. The original model for QHDI consisted of a baryon field ψ of mass m_N coupled to a scalar meson (σ) field ϕ of mass m_s and coupling constant g_s, and a vector meson (ω) field V_μ of mass m_v and coupling constant g_v.

MFT and RHA correspond to adopt the tadpole graph of Fig. 2(a) in Σ_N [25]. The difference between MFT and RHA is that in the first approach only the contributions from nucleons in the filled Fermi sea are retained in the evaluation of the present N loop. Effective mass and single particle energy read $\tilde{m}_N \equiv m_N^* = m_N + \Sigma^s$, $\tilde{E}(\mathbf{p}) \equiv (E^*(\mathbf{p}) \equiv \sqrt{m_N^{*2} + \mathbf{p}^2}) - \Sigma^0$, $\Sigma^0 = -\frac{g_v^2}{m_v^2}\rho_A$. There are dif-
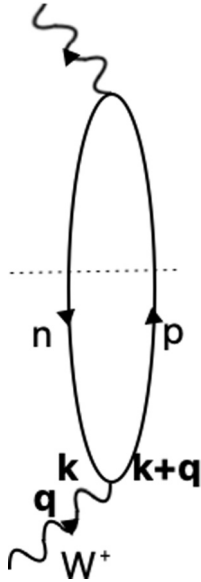
ferent expressions for the nuclear matter energy density $\mathcal{E}_{\mathrm{MFT,RHA}}(\frac{g_s^2}{m_s^2}, \frac{g_v^2}{m_v^2}, m_{N^*})$, due the mentioned different tadpole evaluations. Then, by the minimizing the condition $\frac{\partial\mathcal{E}_{\mathrm{MFT,RHA}}}{\partial m_N^*} = 0$ and together the equilibrium property $\frac{\mathcal{E}A - m_N A}{A}\big|_{k_F} = -15.75$ MeV we fix $\frac{g_s^2}{m_s^2}, \frac{g_v^2}{m_v^2}$ and m_N^*. From the above discussion it is clear that in the effective mass we incorporate the binding of the nucleons.

When the cross graph of Fig. 2(b) is included, we get the RHF approximation with solutions $\tilde{E}(\mathbf{p})$ and m_N^* close to MFT results at normal density. The values $m_N^* = 0.56 m_N$, $\Sigma^0 = -300$ MeV were obtained in the MFT and RHF approaches (see Ref. [25]) while within the RHA approach one gets $m_N^* = 0.73 m_N$, $\Sigma^0 = -180$ MeV.

An important question is in order. Should we use the effective mass $\tilde{m}_N < m_N$ also in the hadron current operator $\hat{J}_H^\mu$ (see Appendix) or not? If yes, we should have an enhancement of the anomalous N magnetic moment inside the nucleus, and consequently as was shown in Ref. [23] for 500-MeV electron scattering data, the agreement with the cross section is not possible. However, we can think that the effective mass is an approximated way to introduce interaction effects in the N wave function, while the current operator is the same as for free nucleons in the spirit of the impulse approximation. Now, it is possible to describe QE scattering very well [23]. Of course, this numerical agreement does not provide a convincing justification of our choice. The main difficulty is that, to answer the question definitely, we must be able to calculate the electromagnetic form factors $F_{1,2}$. This is clearly beyond the range of the simple field theory we have used as it assumes pointlike nucleons. To be more precise, nucleons become "dressed" by a surrounding cloud of scalar and vector mesons but this is not sufficient of course to explain the observed N structure.

FIG. 1. QE 1p1h response for ν scattering. For $\bar{\nu}$ scattering we change $n, p, W^+ \to p, n, W^-$. Here, the W boson emitted from the weak vertex is absorbed by $N = n, p$ from the 0p0h component of GS and excited above the Fermi level.
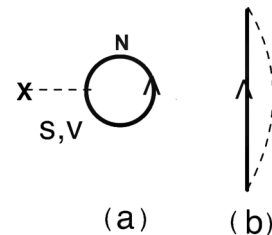

FIG. 2. Self-energy contributions in the QHDI. With dashed lines we indicate the scalar (s) and vector (v) meson exchange.
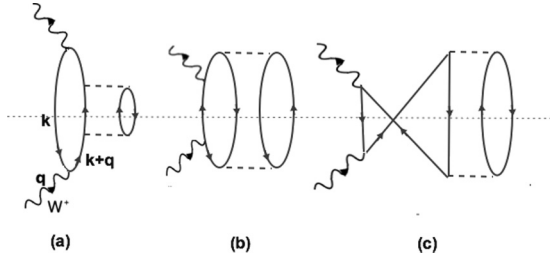
FIG. 3. 2p2h and 3p3p final states from FSI and GSC contributions are shown. (a) 1p1h excitation generated on the 0p0h GS component and then FSI generate an additional ph pair; (b) and (c) the action on a 2p2h GS component. In (b) hole or particle scattering leads to 2p2h final states while in (c) an additional 1p1h excitation is produced to get 3p3h final states. Interference contributions between excitation amplitudes from (a) and (b) are not shown.

On the other hand Ref. [23], independently of the QHDI results described above, kept the bare m_N in the vertex, used Eq. (16) with $\Gamma_N \rightarrow 0$ and $m_{\tilde{N}} = \tilde{m}_{N_f} = m_N^*$ considered as a free parameter, and got the best-fit results for ^{12}C, ^{40}Ca, and ^{208}Pb in 500-MeV QE electron scattering data. A realistic momentum distribution function $n(p)$ was adopted and in the 1p1h energy $E^*(\mathbf{p} + \mathbf{q}) - E^*(\mathbf{p})$, Σ^0 was canceled up. The prescription of using the effective mass also for the final N', is a very simplified form to introduce some kind of FSI. The values $m_N^* = 0.70 m_N - 0.75 m_N$ were obtained, which are much greater than the value $m_N^* = 0.56 m_N$ in the MFT or RHF approach. It is evident only in the interior of the nucleus $m_N^*/m_N \approx 0.56$, but it approaches 1 near the nuclear radius. We may thus conclude that the fitted values $m_N^* = 0.70 m_N - 0.75 m_N$, represent a suitable average over the nucleus. The easiest and most natural way to perform such an average would be the Thomas-Fermi approach [25].

To keep the simpler field theoretical model and taking into account the QHDI and the phenomenological results for m_N^* mentioned above, we assume the RHA approach to treat the QE 1p1h response. Here the mass value is $m_N^* = 0.73 m_N$ and $\Sigma^0 = -180$ MeV, and we have $\tilde{E}(\mathbf{p}) \approx \sqrt{\mathbf{p}^2 + m_N^{*2}}$ that led to $m_N^{*'} \approx 880$ MeV while $\Gamma_N \rightarrow 0$ (because $\text{Im} \Sigma_N^{RHA} = 0$). Finally, as $\text{Re}[\Sigma_N^{RHA}]$ is constant and from (11) $Z_\mathbf{p}^+ = 1$, we have $n(p) = Z_\mathbf{p}^+ \theta(k_F - p) = \theta(k_F - p)$. In summary, within this approach $\Sigma_N \approx \Sigma_{RHF}$ we finally treat with the form Eq. (4) for the propagator but with effective masses through which the binding effect is accounted.

C. 2p2h coming for FSI and GSC

As mentioned in Sec. I, we need to add the contribution of 2h2h, 3p3h, etc., excitations to describe the MiniBoone data. These have different sources. The FSI interaction of the emerging primary N (excited from the 0p0h component of the GS) with another one in the nucleus generates an additional 2p1h excitation and thus a final 2p2h state, which at the lowest order is shown in the Fig. 3(a). The
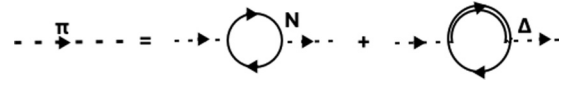

FIG. 4. Pion series modifying π propagation in nuclear matter.

interaction of the W meson with a 2p2h GSC (the 2p2h admixture in the GS) to get by particle-particle (pp), hole-hole (hh), or particle-hole (ph) scattering final 2p2h or 3p3h states, respectively, was schematized in the Born amplitudes of Figs. 3(b) and 3(c). Note the time ordering in the figures.

A word of caution is in order because the imaginary part of the diagram from Fig. 3(a) [and the interference ones between the amplitude excitations from Figs. 3(a) and 3(b)] presents a divergency as we explain here. When placing the 2p2h excitation on the mass shell, we have an intermediate N' unperturbed propagator [see Eq. (4)] with three momentum $\mathbf{k} + \mathbf{q}$, which can be placed on shell for virtual W bosons and we get a pole when $k^0 + q^0 + i\epsilon = E(\mathbf{k}) + q^0 - E(\mathbf{k} + \mathbf{q})$ in the limit $\epsilon \rightarrow 0$. This divergence is not spurious; the Born amplitude represents the probability per unit time of absorbing a virtual W by N (initial) times the probability of collision of N'(intermediate) with other N''(initial) during its lifetime, being ∞ since it became real. This problem was treated within different approaches in the bibliography: (i) by taking an average constant value for $|\mathbf{k}|$, keeping the angular integral over $\hat{\mathbf{k}}$, and adding a constant fictitious width to the N' propagator around of 10 MeV in Ref. [18]; (ii) after a detailed analysis of the problem in Ref. [32], they cured the divergence by a regularization procedure adding a width (within a different interpretation as in Ref. [18]) of around 100 MeV; (iii) by introducing a 2p1h self-energy coming from a NR calculation as in Ref. [33], which would be unsuitable for the large momenta transferred in the experiments under study. It is clear that despite the fact that this contribution is considered small, around 7% for the cross sections and a small shift of the QE peak around 10 MeV, these different procedures could introduce model dependence. Within our model the problem is naturally solved, because we have the perturbed propagator (13) in the amplitude (16), where now the denominator is $p^{02} - \tilde{E}^2 + i\tilde{m}_N \Gamma_N(p)$. The width $\Gamma_N(p)$ is generated by the $\text{Im} \Sigma_N$ relativistic self-energy, now including 2p1h contributions in Fig. 3(a) which give a nonzero value as the difference regarding the RHA.

We will adopt a relativistic self-energy model for Σ_N [29] to add the contribution of Fig. 3(a), which introduces π exchange and maintains at the same time the binding effects introduced in the previous subsection by the σ and ω mesons. In a first step, the MFT is supplemented by the pion π-exchange Fock term similar to Fig. 2(b) (the tadpole one gives zero by parity considerations) modified by π self-energy contributions shown in Fig. 4 and the $\sigma\pi$ interaction, within a chiral-symmetric model [28]. Also, short-range NN, ΔN correlation effects are considered. The minimization of the energy density with respect to m_N^* as before is achieved, and $\frac{g_s^2}{m_s^2}$, $\frac{g_v^2}{m_v^2}$, m_N^* are adjusted (as done in QHDI) so that equilibrium properties may be reproduced. The obtained results for
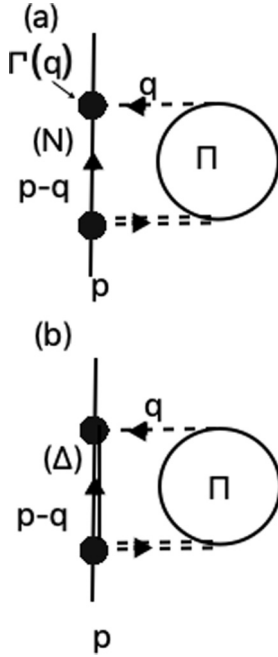
FIG. 5. Contribution to Σ_N that lead to 2p1h contribution. In (a) the TPE not correlated are shown, while in (b) TPE correlated with an intermediate Δ excitation are depicted. At lowest order Π indicates a ph bubble.
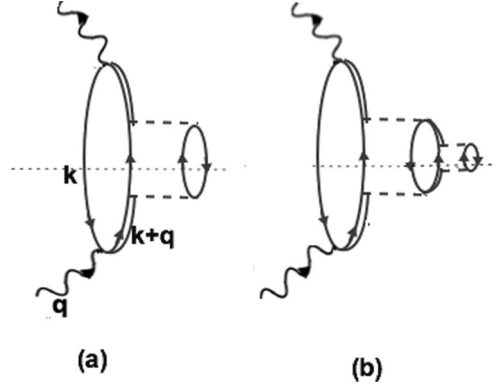

FIG. 6. Δh primary excitation where the Δ decays into 2p1h and 3p2h configurations. The interference amplitude from 2p2h contributions in (a) with those in Fig. 3 coming from FSI are not shown.

the effective mass and Σ^0 were $m_N^* \approx 0.95$, $\Sigma^0 \approx -25$ MeV. Thus, the values obtained in the previous subsection for the RHA were modified by the presence of π.

Then, TPE not correlated from Fig. 5(a) and correlated from Fig. 5(b) are included [29] in Σ_N to generate 2p1h excitations by FSI on the final N'. Now, despite the fact that previously [28] the σ field provided only a small shift of the Dirac mass m_N, the new TPE effects cause an additional shift, that is, 2p1h excitations will have effects on the single particle properties. In addition, the imaginary part of the self-energy coming only from Fig. 5(a) (see [29]) leads to a nonzero Γ_N, preventing divergencies as mentioned above. In summary, we will introduce the FSI between 1p1h and 2p2h final states to all orders and fully relativistically. The proper π self-energy Π in Fig. 5 iterates ph, Δh bubbles and contains the effect of short-range correlations [29]. The calculation gave a value $\text{Re}[\Sigma^s(E_F)] \approx -140$ MeV and $\text{Re}[\Sigma^0] \approx -50$ MeV, which accounts for a value $\tilde{m}'_N = 0.9 m_N$, very close to that of $m_N^{*'} \approx 880$ MeV in RHA. For the imaginary part of the self-energy we adopt the form in Eq. (12) with $-1/2[a^0 - a^s] = 0.11$ obtained by comparison with Ref. [29].

Note that in Eq. (16) because we have functions $\frac{\tilde{m}_N \Gamma(\omega)}{\pi((\omega)^2 - \tilde{E}(\mathbf{p}))^2 + (\tilde{m}_N \Gamma_N(\omega))^2}$ in place of δ sharp ones, we can excite a final N with $\tilde{E}(\mathbf{p} + \mathbf{q}) < E_F$ [suppressed by the factor

$(1 - n(\mathbf{p} + \mathbf{q}))$] from a h (hh scattering) or a p (ph annihilation) belonging to a 2p2h GSC. When $\tilde{E}(\mathbf{p} + \mathbf{q}) > E_F$ we have pp scattering from a 2p2h GSC or ph creation from the 0p0h GS component. The contribution in Fig. 5(b) enables the contribution of Δhph admixtures in the GS participating in hh scattering. In Ref. [29], the Δ intermediate state [Fig. 5(b)] does not contribute to $\text{Im}\Sigma_N$ nor the energy dependence of $\text{Re}\Sigma_N$.

Finally, we describe our model for the momentum distribution $n(p)$. As mentioned at the end of Sec. II A, Z_p^+ determines $n(p)$ and depends on Σ_N through Eq. (11). To get $n(p)$ from this scheme is not a trivial task. In place of this, we will assume an independent model for it. This was used in other calculations [23,26,27] with consistent results. The distribution to be used was built from a perturbative calculation in nuclear matter for a GS within 0p0h, 2p2h, and 4p4h configuration space, which is the minimum one in order for the cancellation with disconnected norm contributions to be complete, avoiding extensive effects in nuclear matter [30]. The NN force employed contains exchange of mesons and short-range correlations within a Landau-Midgal parametrization.

D. $\Delta \to$ 2p2h, 3p3h contributions

The alternative way of getting 2p2h (and also 3p3h) states, is after a primary $WN \to \Delta$ excitation when the Δ decays into 2p1h or 3p2h configurations, by absorption of the emitted virtual π. These contributions to $\mathcal{M}$ in Eq. (2) are shown in Figs. 6(a) and 6(b), respectively. They are incorporated into the resonance self-energy and thus in its width, that also contains the main $\Delta \to \pi N$ decay leading to a final real π (not considered here).

We consider the Δh intermediate state in Eq. (2). In the Appendix we define this contribution and the following

similar steps in getting Eq. (16); we now obtain

$$2\text{Im}\sum_{m_{\nu,I}}\mathcal{M}_{\Delta h} = \frac{8}{(2\pi)^5}\left(\frac{G_F}{\sqrt{2}}\right)^2\cos^2\theta_C\int dk^3\sum_I(\sqrt{2})^2C_I^2\int m_l d\cos\theta_l dE_l \mathrm{p}_l d\Phi_l \tilde{m}_N\frac{L^{\beta\alpha}}{m_l}$$

$$\times \int_{\omega_{\min}}^{E_F}d\omega\sum_{m_s}\left[\bar{u}(\mathbf{k},m_{s_1})\gamma_0\widehat{J}_{\Delta\beta\mu}(q)^\dagger\gamma_0 P^{\mu\nu}(k+q)\widehat{J}_{\Delta\nu\alpha}(q)u(\mathbf{k},m_s)\right]$$

$$\times \frac{(-i)}{\pi}\text{Im}\left[\frac{1}{(k+q)^2-m_\Delta^2+i\Gamma_\Delta m_\Delta}\right]\frac{\tilde{m}_N\Gamma(\omega)n(\mathbf{k})}{\pi[((\omega)^2-\tilde{E}(\mathbf{k}))^2+(\tilde{m}_N\Gamma_N(\omega))^2]}, \tag{17}$$

where we must sum over isospin states because for ν and $\bar{\nu}$ we can excite on a n a $\Delta^{+,-}$, while on a p a $\Delta^{++,0}$, respectively. Note that the $P^{\mu\nu}$ (defined in the Appendix) is consistent from the point of view of contact transformations with the usually assumed $\Delta\pi N$ vertex $\frac{f_{\pi N\Delta}}{m_\pi}p_\pi^\mu$, but not with its on-shell contribution obtained by making $\not{p}=m_\Delta$ in the off-shell term. $P^{\mu\nu}(p)$ is in this case denominated on the on-shell spin 3/2 projector [36]. This is a common mistake, present in several other models that can lead to a different evaluation for the Δ contribution because the dropped term grows as $p^2 > m_\Delta^2$. For the width we use the model of Ref. [37], where it is analyzed how to introduce Δ self-energy to account for 2p2h+3p3h effects. The Γ_Δ will be calculated as follows:

$$\Gamma_\Delta = \Gamma_\Delta^{\text{free}} - \Delta\Gamma_\Delta^{\text{Pauli}} + \Gamma_{2p2h+3p3h}, \tag{18}$$

where the lowest order contribution of the 2p2h and 3p3h to the Δ decay are shown schematically in Figs. 6(a) and 6(b), while the $\Gamma_\Delta^{\text{free}}$ is obtained from πN decay in the free space. The other contributions are the Pauli-blocking contribution, coming from the fact that when the resonance decays within the nucleus, the N is Pauli blocked. We have fitted a second-order polynomial to the results in [37]

$$\Gamma_{2p2h+3p3h}(q_0) = -2\text{Im}\Sigma_{2p2h+3p3h}(q_0)$$
$$= [40 - 4\times10^{-4}\times(q_0-350)^2]$$
$$\times\theta(600-q_0)+16\theta(q_0-600),$$
$$\Delta\Gamma_{\text{Pauli}}(q_0) = -2\text{Im}\Sigma_{\text{Pauli}}(q_0)$$
$$= 48.30\theta(q_0-440)+0.8(0.23q_0$$
$$-40.8)\theta(440-q_0). \tag{19}$$

For the bare value $\Gamma_\Delta^{\text{free}}$ we assume that obtained within the complex mass scheme (CMS) in our previous works [34,35] on weak π production, and for m_Δ we assume the effective value $\tilde{m}_\Delta \equiv m_\Delta - (1-\frac{\tilde{m}_N}{m_N})m_N$ which is known as the universality approach [38]. Note that we have not made the substitution $m_\Delta \to m_\Delta - i\frac{\Gamma_\Delta}{2}$ on the unperturbed $G_{\mu\nu}^0 = G_{\mu\nu}(\Gamma_\Delta=0)$ in every place as required by the CMS, only in the $p^2-m_\Delta^2$ denominator and thus $P_{\mu\nu}$ is not affected. To these considered energies, this approach should work well. For this, we only take the imaginary part of $\frac{1}{(k+q)^2-m_\Delta^2+i\Gamma_\Delta m_\Delta}$ and we keep the full Γ_Δ from (19) in the denominator but only $\Gamma_{2p2h+3p3h}$ in the numerator to consider only the 2p2h+3p3h channel decay. Finally, we will discuss in the next section the contributions of the interference between 2p2h amplitudes coming from a primary N (FSI or GSC) with those from Δ decay, as well as the two-body MEC as PF, CT, and PP.

III. CALCULATIONS AND RESULTS

In the beginning, only the total cross section as a function of the ν and $\bar{\nu}$ energy was evaluated and compared with the so-called "unfolded" data in Refs. [12,13]. The experimental data include energy and angle distributions, and therefore provide more complete information. Furthermore, the unfolded total cross section is not a very clean observable after discovering the importance of multinucleon mechanisms, because the unfolding itself is model dependent and assumes that the events are purely QE [39]. The same limitation occurs for the differential cross section, $d\sigma/dQ^2$, given that Q^2 comes assuming only QE events. Thus, the proper observable to contrast theoretical models, and to constrain free parameters, is the double differential cross section $d^2\sigma/dT_\mu d\cos\theta_\mu$ because both the final lepton angle and energy are directly measured. In addition, the uncertainties linked to the fact that the neutrino spectrum is broad are of experimental origin because the extraction of the energy dependence of the cross section involves a reconstruction of the neutrino energy, whereas in the theoretical evaluation the neutrino energy is just an input. The double differential cross section is free from the uncertainty of neutrino energy reconstruction. However, it remains a theoretical uncertainty because the measured double differential cross section corresponds to the broad flux of neutrino energies. Theoretical predictions needs a convolution with this flux, defined as

$$\frac{d\sigma^2}{dT_l d\cos\theta_l} \equiv \left\langle\frac{d\sigma_{\nu A}^2}{dT_l d\cos\theta_l}\right\rangle = \frac{1}{\int\Phi(E_\nu)dE_\nu}$$
$$\times \int dE_\nu\frac{d\sigma_{\nu A}^2}{dT_l d\cos\theta_l}|_{E_\nu(T_l,\cos\theta_l)}\Phi(E_\nu),$$

where the flux is obtained from the experiments in Refs. [12,13], and could be a source of error. Nevertheless, a good agreement with theory for the double differential cross section supports the idea of multinucleon emission process. For the QE FF we assume

$$F_1^V = \frac{1}{2}\left[1+(2.79+1.91)\frac{Q^2}{4m_N^2}\right]\frac{1}{1+\frac{Q^2}{4m_N^2}}\frac{1}{\left(1+\frac{Q^2}{0.71}\right)^2},$$

$$F_2^V = \frac{1}{2}[1.79+1.91]\frac{1}{\left(1+\frac{Q^2}{0.71}\right)^2},$$
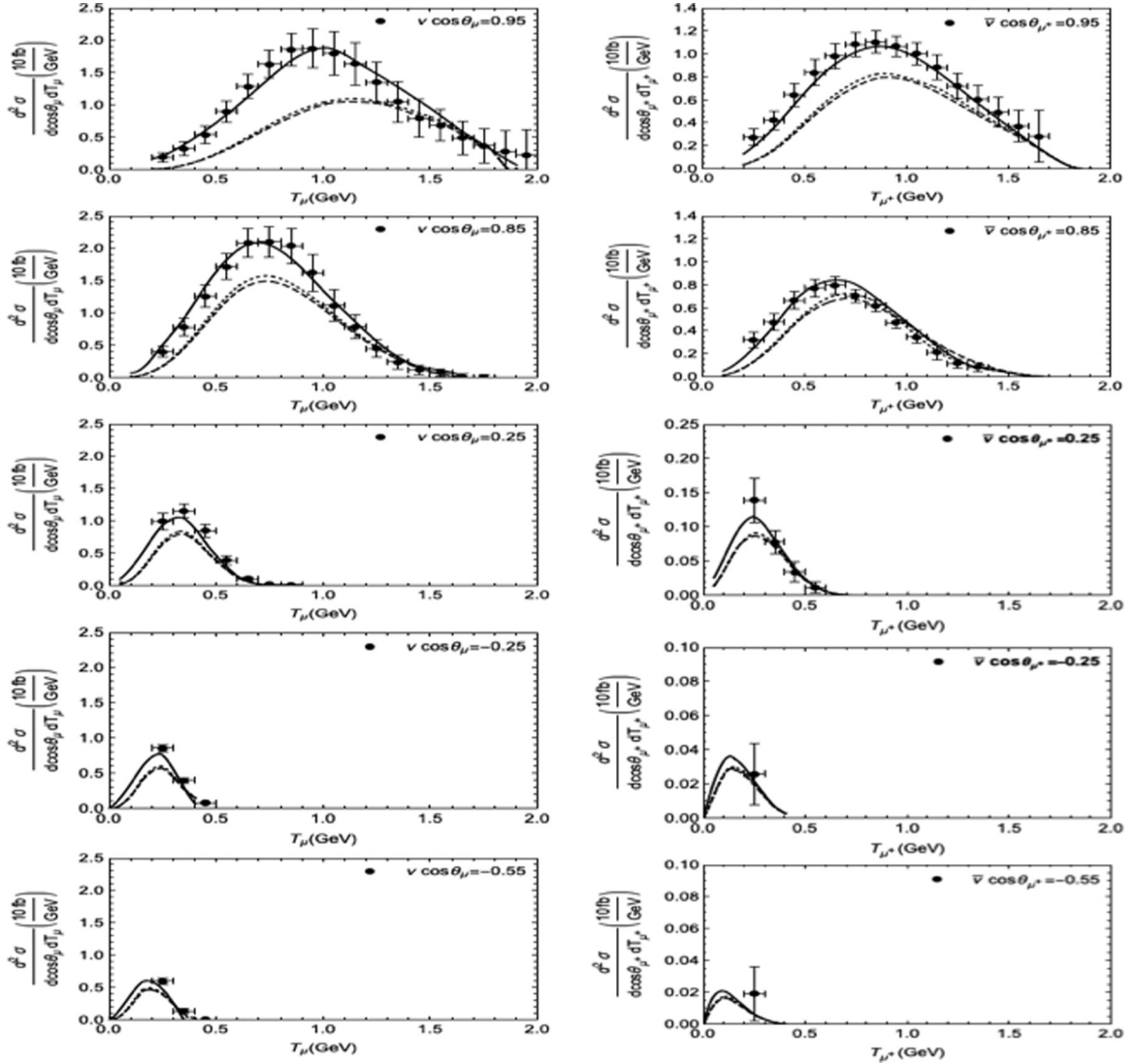
$$G_A = \frac{1.26}{1+(Q^2/1.032^2)},$$

FIG. 7. Left (right) panel double differential cross section for $\nu(\bar{\nu})$ scattering at certain $\cos\theta_\mu(\cos\theta_{\mu^+})$ selected bins. With dotted lines QE 1p1h response within the RHA is indicated. Dashed lines indicate QE 1p1h + 2p2h (coming from FSI and GSC). Finally full lines also include the Δh excitations that decay into 2p2h and 3p3h final states. Data are obtained from the MiniBooNE experiment of Refs. [12,13].

as in our previous work [34], where the axial parameters for the Δ were determined, and use $\tilde{m}'_N = 0.9 m_N$, $\tilde{m}'_{Nf} = 0.80(0.85)$ for $\nu(\bar{\nu})$ scattering.

We are going to calculate the unfolded and folded cross section using the model described in the previous sections that is fully relativistic within the frame of QHDI [25] with primary one-body currents exciting nucleons and isobar Δ. It introduces FSI through a relativistic self-energy that enclose correlated and uncorrelated TPE with GSC introduced through a realistic nucleon momentum distribution calculated in the basis of 0p0h, 2p2h, and 4p4h configurations for the GS. We use the Lehmann representation for the nucleon propagator which leads to the expressions (16) and (17), where the width in the nucleons enables ph, hh, pp, and hp excitations, generated on the different components of the GS. Also, the contribution shown in Fig. 5(b) with the hh scattering, enables contributions with Δh admixtures in the GS. We show in

Fig. 7 the double differential cross sections for ν and $\bar{\nu}$ scattering for different selected bins for the $\cos\theta_{\mu,\mu^+}$ as a function of T_{μ,μ^+} energies. The left panel corresponds to ν scattering while the right one to $\bar{\nu}$ scattering.

The dotted lines correspond to introduce only the contribution (16) in (2) and (1), making $\Gamma_N \to 0$, and $n(k) \to \theta(k_F - k)$, this corresponding to the RHA (close to the relativistic Fermi gas model). As it is well known, the data are underpredicted in this case. When the self-energy contributions of Fig. 5 are considered and the correlated $n(\mathbf{k})$ is used, several effects are illuminated. First, as mentioned previously, a small change in $\tilde{m}'_N$ is accounted for. Then, FSI of the emitted nucleons, Fermi smearing effects together with the ph, pp, hh, hp, and Δh excitations because of the smooth weights for the $E(\mathbf{k})$ and $E(\mathbf{k} + \mathbf{q})$ single particle states around E_F, are composed to give small effects resulting in a very tiny energy shift and diminishing the cross section. It is important
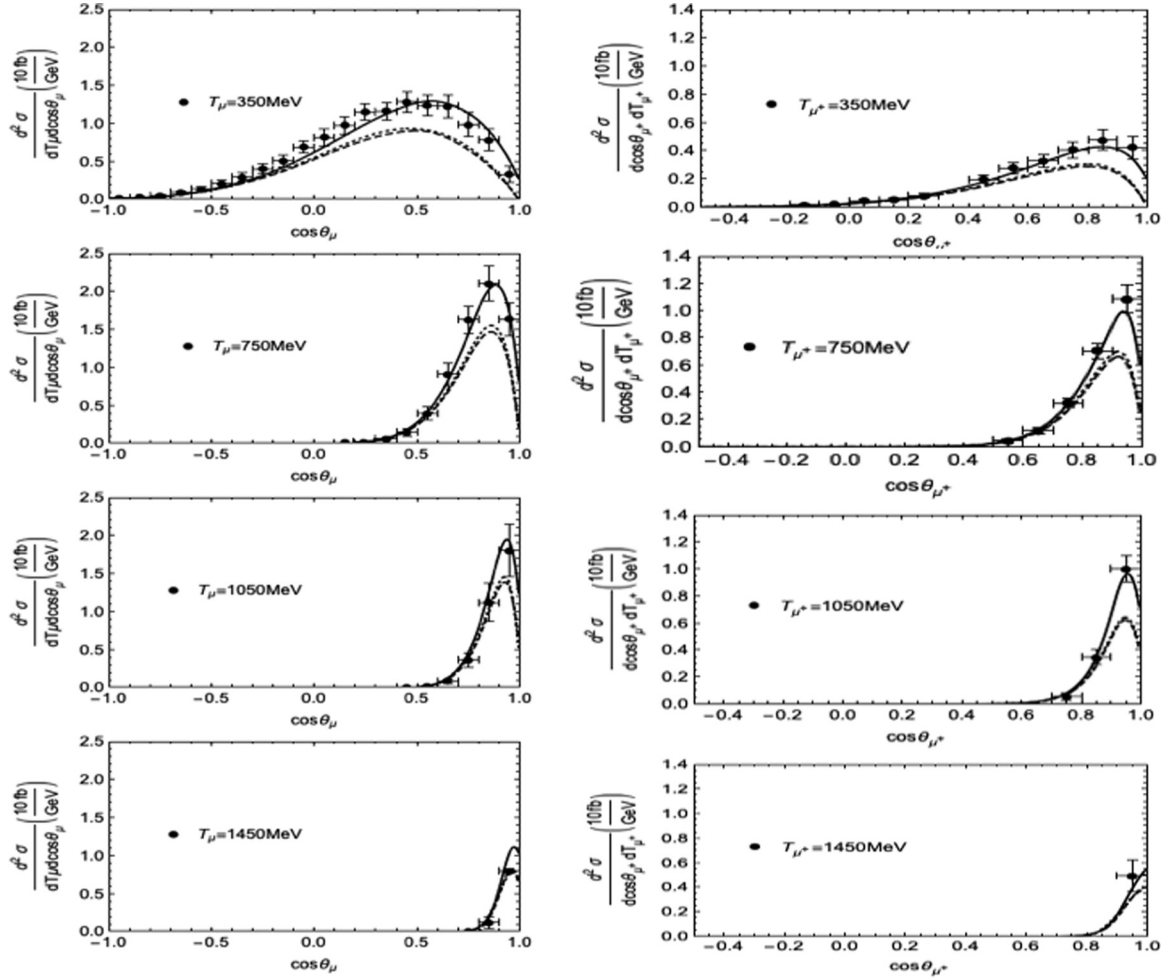
FIG. 8. Left (right) panel double differential cross section for $\nu(\bar{\nu})$ scattering at certain $T_\mu(T_{\mu^+})$ selected bins. Descriptions of lines and data are the same as in Fig. 7.

to stress that all these effects must be considered together because, as described in Sec. II, GSC are lighted on when 2p1h are considered in Σ_N. These results have the tendency of the comparison between the bare QE and QE+RPA achieved in Refs. [14,18] but with a much minor diminishing effect perhaps by the pp and hh contributions, coming for 2p2h plus 4p4h GS correlations. Nevertheless, an observation should be done. To account for the contributions of 2p2h excited states from N in all possible ways, the $WN \rightarrow N'\pi$ amplitude with N intermediate states is added to $\hat{J}_H^\mu(q)$ in Ref. [18]. Then, π is absorbed producing an additional ph state. In addition to the CT, PF, and PP contributions, that in combination with the produced ph are considered two-body MEC (we do not enclose the amplitudes with Δ's within this category in spite of the fact that other authors do; see Ref. [20]), the one nucleon pole (NP) and nucleon cross (NC) can generate all our contributions mentioned above in our model. The difference is that N and N' are not weighted by a correlated momentum distribution which accounts for the depletion and the structure of the GS, because $n(p) = \theta(p)$. This should lead to a different value for such induced contributions. The same cross sections, except for different bins of the T_{μ,μ^+} energies

as a function of $\cos\theta_{\mu,\mu^+}$, are shown in Fig. 8 with a similar behavior for the above mentioned RHA and with the nucleon self-energy effects. When the Δh amplitude from Eq. (17) is considered in Eqs. (2) and (1), the full line is obtained, showing a good coincidence with the data both for ν and $\bar{\nu}$ for the different cuts in the cross sections. Here, also we have the weight of the correlated momentum distribution on the h states in (17). Also, as mentioned in the previous section, we are adopting a consistent treatment for the Δ amplitude [34].

To be precise we must mention that we are omitting two kinds of contributions: those from the interference of the 2p2h amplitudes coming from the decay of a primary ph, and those coming from the decay of a Δh one. These contributions have been evaluated in Ref. [14] giving a contribution around 1.5%, which does not alter our conclusions. These contributions were omitted because now we need to evaluate a contribution like that of Fig. 6(a) but replacing the primary Δ by N, and to avoid the above mentioned singularity with its propagator, the dressed one should be replaced by the bare one. Also, in that contribution Δ has a width as that described in Eq. (18). Then, it is not clear how consistency is achieved because the π loop
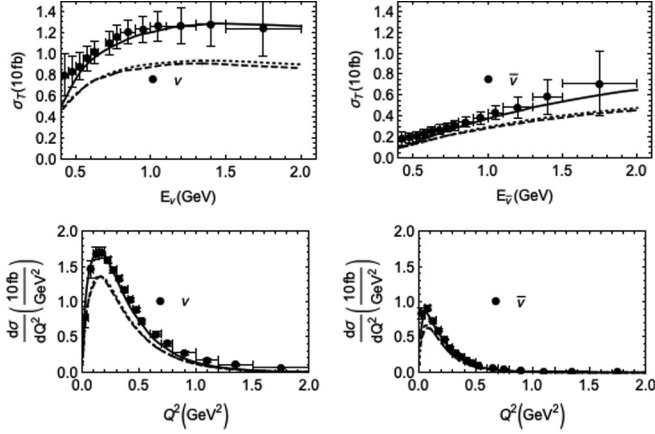
FIG. 9. Total unfolded and folded $d\sigma/dQ^2$ cross sections. Descriptions of the lines and data are the same as in Fig. 7.
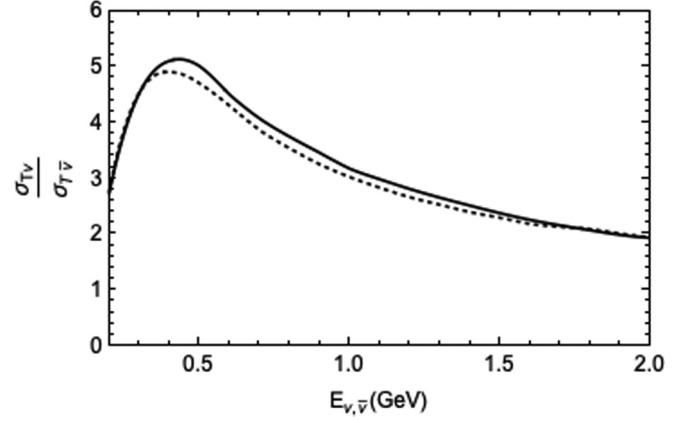

FIG. 10. Ratio of total unfolded cross sections of neutrinos over antineutrinos for the QE 1p1h(dashed) approach and full with QE+npnh contributions (full lines).

involved in this contribution should be calculated with the same approach that was used n both the $\Gamma_{N,\Delta}$ widths, which is not a trivial or possible task. The other thing that we are not including is the two-body MEC involving the nucleon, the above mentioned CT, PF, and PP contributions. From our previous calculation on π production in νN scattering in Ref. [34], CT, PF, and PP amplitudes contribute around 5%–9% of the total π-production cross section. Calculations done with the same model give for $\bar{\nu}N$ around 1.5%–10%. As the total π-production contribution induces around 30%(ν)–40%($\bar{\nu}$) of increase regarding the QE 1p1h cross section, because the emitted π is what generates additional final nucleons, when MEC are considered we await a contribution around 1.5%–2.7%(ν) and 0.6%–4%($\bar{\nu}$). For this reason, we keep us within an approach only with one-body currents and reserve the two-body MEC CT, PF, and PP for a future refinement.

Finally, results for the unfolded total $\sigma(E_{\nu,\bar{\nu}})$ and folded $d\sigma/dQ^2$ are shown in Fig. 9. As can be seen the same behavior as in the double differential cross section is confirmed, with a very small underprediction for $d\sigma_{\bar{\nu}}/dQ^2$ and the total $\sigma(E_{\bar{\nu}})$ around 5% which could be as a consequence of our simplifications.

The total cross section was analyzed also in the antineutrino mode by Martini *et al.* [15], Nieves *et al.* [18] and Bodek *et al.* [21]. The effect of npnh in the ratio $\sigma(E_\nu)/\sigma(E_{\bar{\nu}})$ is compared to one nucleon ejection QE case. This effect should be somewhat less important for $\bar{\nu}$ because the spin-isospin response which is affected by the 2p2h piece has less weight for antineutrino, owing to the negative axial-vector interference. This effect is evident in Martini *et al.* and Bodek *et al.*, and not so much in Nieves *et al.*, where the ratio shows a value around 5% of more contributions for $\bar{\nu}$. Our results shown in Fig. 10 agree with the tendency of Refs. [15,21], with 4% greater for ν in regard to $\bar{\nu}$ regarding the QE case. In Ref. [18], the relative higher importance of the npnh contributions for $\bar{\nu}$ scattering is justified mainly by the effects induced by the CT and PP terms that help increase it. Nevertheless, because of the size

of these contributions we think that our approach should help the QE+npnh ratio approach the QE one.

IV. CONCLUSIONS

We have implemented a new model to study ν and $\bar{\nu}$ scattering on nucleus that enables one to introduce npnh contributions to the QE response, fully relativistically and consistently. We work within a quantum hydrodynamics nuclear matter frame, producing QE ph excitations and Δh excitations through one-body meson exchange currents. We begin with the RHA approach, and then to introduce FSI in a relativistic fashion, we include pion ring series and TPE correlated and uncorrelated in the nucleon self-energy. In this way, FSI on the emerging nucleon are introduced to all orders avoiding the mentioned singularity problem in the Born amplitudes. The nucleon propagator is introduced through the Lehmann representation, which enables us to treat FSI and GSC on the same footing. GSC are also introduced through a realistic nucleon momentum distribution that results adequately for the nuclear matter frame. The Δ excitation is introduced consistently, regarding the adopted $\pi N \Delta$ vertex and Δ propagator. We add 2p1h and 3p2h contributions to the Δ self-energy, because the emitted pion from its decay can excite another ph excitation. Coincidently the data are good and it seems that the descriptions of both ν and $\bar{\nu}$ are consistent. We think that this is a step ahead, considering the simplicity of the model. As we have discussed above, many improvements should be achieved to introduce some interference terms and CT, PP, and PF MEC, consistent with a correlated nucleon propagator. Nevertheless, we have given arguments to show that these effects do not affect our results. Despite this, we plan to include them in a future calculation.

APPENDIX

In this Appendix we show the basic expressions from where amplitudes are obtained. The amplitude (16), that corresponds to the Fig. 1 is built by using the corresponding Feynman rules and reads

$$2\text{Im}\sum_{m_\nu}\mathcal{M}_{1p1h} = 2\sum_{m_\nu}\int\frac{dp_l^4}{(2\pi)^4}\bar{u}(k_\nu m_\nu)(-i)\gamma_0[\gamma^\beta(1-\gamma_5)]^\dagger\gamma_0 iS_l(p_l)(-i)\gamma^\alpha(1-\gamma_5)u(k_\nu, m_\nu)$$

$$\times i^2\left(\frac{g}{2\sqrt{2}M_W}\right)^4\cos^2\theta_c\text{Im }i\int\frac{dk^4}{(2\pi)^4}\text{Tr}[(-i)\gamma_0\widehat{J}_{H\beta}(k, q)^\dagger\gamma_0 iS_N(k+q)(-i)\widehat{J}_{H\alpha}(k, q)iS_N(k)], \quad \text{(A1)}$$

where $u(k_\nu, m_\nu)$ is the neutrino spinor, $S_l(p_l) = \frac{\not{p}_l+m_l}{p_l^2-m_l^2+i\epsilon} = \frac{\not{p}_l+m_l}{(p_l^0-E_l+i\epsilon)(p_l^0+E_l-i\epsilon)}$ the lepton propagator, $V_{ud}^2 = \cos^2\theta_c$ and $G_F/\sqrt{2} = g^2/8M_W^2$. We use the N perturbed propagator S_N in the representation defined by Eqs. (7) and (15) to include the contributions in Fig. 3. Finally we have the weak vertex,

$$\hat{J}_H^\mu(q) = \frac{-i}{2}\left[F_1^V(q^2)\gamma^\mu + i\frac{F_2^V(q^2)}{2m_N}\sigma^{\mu\nu}q_\nu - F_A(q^2)\gamma^\mu\gamma_5\right](W\cdot\tau), \quad \text{(A2)}$$

W being the isospin wave function of the W boson, and the isospin factors read

$$\langle p/n|W^\pm\cdot\tau|n/p\rangle = \mp\sqrt{2}. \quad \text{(A3)}$$

Now, we choose to integrate in (A1) p_l^0 clockwise in the lower complex plane, while k^0 is counterclockwise in the upper one by using the Cauchy's residue theorem. Then, we use the N spinor relation $\sum_{m_s}u(k, m_s)\bar{u}(k, m_s) = \frac{\not{k}+m_N}{2m_N}$ with $k = (\omega, \mathbf{k})$ and spin and trace identities,

$$\sum_{m_\nu}u(k_\nu, m_\nu)\bar{u}(k_\nu m_\nu) = \not{k}_\nu,$$

$$\tfrac{1}{8}\text{Tr}[\not{k}_\nu\gamma^\beta(1-\gamma_5)(\not{p}_l+m_l)\gamma^\alpha(1-\gamma_5)] = \left[k_\nu^\alpha p_l^\beta + k_\nu^\beta p_l^\alpha - g^{\alpha\beta}k_\nu\cdot p_l \mp i\epsilon^{\delta\beta\lambda\alpha}p_{l\delta}k_{\nu\lambda}\right] \equiv L^{\beta\alpha},$$

where the $-$ sign corresponds to ν while $+$ to $\bar{\nu}$. After doing all these steps the final Eq. (16) is obtained.

Replacing $S_N(k+q)$ by the Δ propagator $G^{\mu\nu}(k+q)$ and the corresponding hadronic vertex $\widehat{J}_H^\alpha$ by $\hat{J}_\Delta^{\nu\alpha}$in Eq. (A1), we get the Δh amplitude in Eq. (2) as

$$2\text{Im}\sum_{m_{\nu,I}}\mathcal{M}_{\Delta h} = 2\sum_I C_I^2\sum_{m_\nu}\int\frac{dp_l^4}{(2\pi)^4}\bar{u}(k_\nu m_\nu)(-i)\gamma_0[\gamma^\beta(1-\gamma_5)]^\dagger\gamma_0 iS_l(p_l)(-i)\gamma^\alpha(1-\gamma_5)u(k_\nu, m_\nu)i^2\left(\frac{g}{2\sqrt{2}M_W^2}\right)^2$$

$$\times\cos\theta_C^2\text{Im }i\int\frac{dk^4}{(2\pi)^4}\text{Tr}[(-i)\gamma_0\widehat{J}_{\Delta\beta\mu}(k, q)^\dagger\gamma_0\sqrt{2}iG^{\mu\nu}(k+q)(-i)\widehat{J}_{\Delta\nu\alpha}(k, q)\sqrt{2}iS_N(k)], \quad \text{(A4)}$$

where the currents are $\widehat{J}_{\Delta\nu\alpha}(k, q) = \widehat{\mathcal{J}}_{\Delta\nu\alpha}(k, q)(T^\dagger\cdot W)$, $\widehat{\mathcal{J}}_{\Delta\nu\alpha}$ being defined in Refs. [34,35] where we worked in the Sachs parametrization for the vector part. In Eq. (A4) we have the Δ propagator $G^{\mu\nu} = \frac{1}{(k+q)^2-m_\Delta^2+i\Gamma_\Delta m_\Delta}P^{\mu\nu}$ where

$$P^{\mu\nu}(p) = (\not{p}+m_\Delta)\left\{-g^{\mu\nu} + \frac{1}{3}\gamma^\mu\gamma^\nu + \frac{2}{3m_\Delta^2}p^\mu p^\nu - \frac{1}{3m_\Delta}(p^\mu\gamma^\nu - \gamma^\mu p^\nu)\right.$$

$$\left. - \frac{2(\not{p}-m_\Delta)}{2m_\Delta^2}[\gamma^\mu p^\nu - p^\mu\gamma^\nu + (\not{p}+m_\Delta)\gamma^\mu\gamma^\nu]\right\}, \quad \text{(A5)}$$

where the last term is usually called off-shell contribution because it grows as $p^2 - m_\Delta^2$.

For the isospin coefficients we have $(\sqrt{2}\langle\Delta^+, \Delta^{++}|T^\dagger\cdot W^+|n, p\rangle)^2 = \sqrt{2}^2 C_I^2 = 2, 2/3$, and because

$$\langle\Delta^0, \Delta^-|T^\dagger\cdot W^- \equiv T_-^\dagger|p, n\rangle = \langle T=3/2, M_T = -1/2, -3/2|T_-^\dagger|T=1/2, M_T = 1/2, -1/2\rangle$$

$$= \frac{\langle 3/2||T^\dagger||1/2\rangle}{\langle 1/2; 1/2, -1/2; 1-1|3/2; -1/2, -3/2\rangle}$$

$$= \frac{\langle 3/2||T^\dagger||1/2\rangle}{\pm\langle 1/2; -1/2, 1/2; 1+1|3/2; 1/2, +3/2\rangle}$$

$$= \pm\langle\Delta^+, \Delta^{++}|T^+|n, p\rangle = \mp\langle\Delta^+, \Delta^{++}|T^\dagger\cdot W^+|n, p\rangle,$$

and for squared we have no difference between ν and $\bar{\nu}$ scattering. After doing similar steps described above for the ph case, we get Eq. (17).

[1] We follow the conventions of J. D. Bjorken and S. D. Drell, *Relativistic Quantum Mechanics* (McGraw-Hill, New York, 1964).

[2] C. F. Perdrisat, V. Punjabi, and M. Vanderhaeghen, Prog. Part. Nucl. Phys. **59**, 694 (2007).

[3] V. Bernard, L. Elouadrhiri, and U. G. Meissner, J. Phys. G **28**, R1 (2002); V. Lyubushkin *et al.*, Eur. Phys. J. C **63**, 355 (2009).

[4] A. Bodek, S. Avvakumov, R. Bradford, and H. S. Budd, Eur. Phys. J. C **53**, 349 (2008).

[5] L. Alvarez-Ruso *et al.*, Prog. Part. Nucl. Phys. **100**, 1 (2018).

[6] MicroBooNE Experiment, [http://www-microboone.fnal.gov].

[7] NOvA Experiment, [http://www-nova.fnal.gov].

[8] T2K Experiment, [http://t2k-experiment.org].

[9] MINER nA Experiment, [http://minerva.fnal.gov].

[10] Deep Underground Neutrino Experiment, [http://www.dunescience.org].

[11] Hyper-Kamiokande, [http://www.hyperk.org].

[12] A. A. Aguilar-Arevalo *et al.* (MiniBooNE Collaboration), Phys. Rev. D **81**, 092005 (2010).

[13] A. A. Aguilar-Arevalo *et al.*, Phys. Rev. D **88**, 032001 (2013).

[14] M. Martini, M. Ericson, G. Chanfray, and J. Marteau, Phys. Rev. C **80**, 065501 (2009); **81**, 045502 (2010).

[15] M. Martini, M. Ericson and G. Chanfray, Phys. Rev. C **84**, 055502 (2011); M. Martini and M. Ericson, *ibid.* **87**, 065501 (2013).

[16] J. E. Amaro, M. B. Barbaro, J. A. Caballero, T. W. Donnelly, and J. M. Udías, Phys. Rev. D **84**, 033004 (2011); J. E. Amaro, M. B. Barbaro, J. A. Caballero, T. W. Donnelly, and C. F. Williamson, Phys. Lett. B **696**, 151 (2011).

[17] G. D. Megias, J. E. Amaro, M. B. Barbaro, J. A. Caballero, T. W. Donnelly, and I. R. Simo, Phys. Rev. D **94**, 093004 (2016).

[18] J. Nieves, I. Ruiz Simo, and M. J. Vicente Vacas, Phys. Rev. C **83**, 045501 (2011); Phys. Lett. B **721**, 90 (2013); **707**, 72 (2012).

[19] J. E. Sobczyk, J. Nieves, and F. Sánchez, Phys. Rev. C **102**, 024601 (2020).

[20] N. Rocco, C. Barbieri, O. Benhar, A. De Pace, and A. Lovato, Phys. Rev. C **99**, 025502 (2019).

[21] A. Bodek, H. Budd, and M. E. Christy, Eur. Phys. J. C **71**, 1726 (2011).

[22] W. M. Alberico, M. Ericson, and A. Molinari, Ann. Phys. **154**, 356 (1984).

[23] R. Rosenfelder, Ann. Phys. **128**, 188 (1980).

[24] L. G. Arnold, B. C. Clark, and R. L. Mercer, Phys. Rev. C **19**, 917 (1979); L. G. Arnold and B. C. Clark, Phys. Lett. B **84**, 46 (1979); M. Jaminon, C. Mahaux, and P. Rochus, Phys. Rev. Lett. **43**, 1097 (1979); H. P. Duerr, Phys. Rev. **103**, 469 (1956).

[25] B. D. Serot and J. D. Walecka, *Advances in Nuclear Physics*, Vol. 16 (Plenum, New York, 1986).

[26] A. Mariano and P. Podesta Lerma, Phys. Rev. C **69**, 034606 (2004).

[27] A. Mariano and C. Barbero, J. Phys. G: Nucl. Part. Phys. **31**, 119 (2005).

[28] H. Jung, F. Beck, and G. A. Miller, Phys. Rev. Lett. **62**, 2357 (1989).

[29] H. Jung and G. A. Miller, Phys. Rev. C **43**, 1958 (1991).

[30] A. Mariano, F. Krmpotic, and A. F. R de Toldedo Piza, Phys. Rev. C **53**, 1664 (1996).

[31] J. P. Jeukenne, A. Lejeune, and C. Mahaux, Phys. Rep. **25**, 83 (1976).

[32] J. E. Amaro, C. Maieron, M. B. Barbaro, J. A. Caballero, and T. W. Donnelly, Phys. Rev. C **82**, 044601 (2010).

[33] J. Nieves, J. E. Amaro, and M. Valverde, Phys. Rev. C **70**, 055503 (2004).

[34] C. Barbero, A. Mariano, and G. L. Castro, Phys. Lett. B **664**, 70 (2008).

[35] A. Mariano *et al.*, Nucl. Phys. A **849**, 218 (2011).

[36] E. Hernandez, J. Nieves, and M. Valverde, Phys. Rev. D **76**, 033005 (2007).

[37] E. Oset and L. L. Salcedo, Nucl. Phys. A **468**, 631 (1987).

[38] M. R. Frank, Phys. Rev. C **49**, 555 (1994); H. Kim, C. J. Horowitz, and M. R. Frank, *ibid.* **51**, 792 (1995).

[39] J. Nieves, F. Sánchez, I. Ruiz Simo, and M. J. Vicente Vacas, Phys. Rev. D **85**, 113008 (2012).